JOURNAL OF BACTERIOLOGY, Oct. 2011, p. 5155–5163 Vol. 193, No. 19
0021-9193/11/$12.00 doi:10.1128/JB.05371-11


# The RpiR-Like Repressor IolR Regulates Inositol Catabolism in *Sinorhizobium meliloti*▽†

Petra R. A. Kohler, Ee-Leng Choong, and Silvia Rossbach*

*Department of Biological Sciences, Western Michigan University, Kalamazoo, Michigan 49008-5410*

Received 20 May 2011/Accepted 14 July 2011

***Sinorhizobium meliloti*, the nitrogen-fixing symbiont of alfalfa, has the ability to catabolize *myo*-, *scyllo*-, and D-*chiro*-inositol. Functional inositol catabolism (*iol*) genes are required for growth on these inositol isomers, and they play a role during plant-bacterium interactions. The inositol catabolism genes comprise the chromosomally encoded *iolA* (*mmsA*) and the *iolY*(*smc01163*)*RCDEB* genes, as well as the *idhA* gene located on the pSymB plasmid. Reverse transcriptase assays showed that the *iolYRCDEB* genes are transcribed as one operon. The *iol* genes were weakly expressed without induction, but their expression was strongly induced by *myo*-inositol. The putative transcriptional regulator of the *iol* genes, IolR, belongs to the RpiR-like repressor family. Electrophoretic mobility shift assays demonstrated that IolR recognized a conserved palindromic sequence (5′-GGAA-$N_6$-TTCC-3′) in the upstream regions of the *idhA*, *iolY*, *iolR*, and *iolC* genes. Complementation assays found IolR to be required for the repression of its own gene and for the downregulation of the *idhA*-encoded *myo*-inositol dehydrogenase activity in the presence and absence of inositol. Further expression studies indicated that the late pathway intermediate 2-keto-5-deoxy-D-gluconic acid 6-phosphate (KDGP) functions as the true inducer of the *iol* genes. The *iolA* (*mmsA*) gene encoding methylmalonate semialdehyde dehydrogenase was not regulated by IolR. The *S. meliloti iolA* (*mmsA*) gene product seems to be involved in more than only the inositol catabolic pathway, since it was also found to be essential for valine catabolism, supporting its more recent annotation as *mmsA*.**

Inositol compounds are present in plants and their rhizospheres (7, 37). Especially high concentrations have been found in legume plants (7, 35). *Sinorhizobium meliloti*, the nitrogen-fixing symbiont of alfalfa, is able to catabolize *myo*-, *scyllo*-, and D-*chiro*-inositol (19). A functional inositol catabolic pathway and the regulatory gene *iolR* are required for successfully competing during host plant nodulation (19). Metabolism of inositol compounds has been linked not only to successful plant-bacterium interactions in members of the *Rhizobiaceae* but also to the survival of the animal pathogen *Brucella* inside its host (9, 11, 15, 21).

The inositol catabolic (*iol*) genes are organized in single clusters in various species of the *Firmicutes* and *Enterobacteriaceae* (3, 17, 20, 36, 39). In contrast, the inositol catabolic genes are dispersed at three different loci in *S. meliloti*. Specifically, the *idhA* gene is located on the pSymB plasmid, while the *smc01163* and *iolRCDEB* genes are clustered together on the chromosome and the *iolA* (*smc00781*) gene is located a further 400 kb away from the *iol* cluster (http://iant.toulouse.inra.fr/S.meliloti).

The proposed inositol catabolic pathway in *S. meliloti* is similar to the pathway in *Bacillus subtilis* (40) (Fig. 1). The initial oxidation of D-*chiro*-inositol ([I] in Fig. 1) and *myo*-inositol ([II] in Fig. 1) in *S. meliloti* is carried out by the *idhA*-encoded *myo*-inositol dehydrogenase, yielding 2-keto-*myo*-inositol (2KMI; [IV] in Fig. 1) (12, 19). Growth with *scyllo*-inositol ([III] in Fig. 1) as the sole carbon source requires the dehydrogenase encoded by the *smc01163* gene (19). The deduced gene product of *smc01163* displays an N-terminal signal peptide, suggesting a periplasmic location. So far, only two other *scyllo*-inositol dehydrogenases have been described from any organisms, namely, IolW and IolX in *B. subtilis* (25). IolW and IolX are probable cytoplasmic enzymes and share limited identity with Smc01163 (26 and 27%, respectively). On the basis of these differences, we suggest annotating *smc01163* as *iolY*. The product of the IolY reaction is probably also 2KMI (19). The further degradation of 2KMI requires the *iolE*, *iolD*, *iolB*, *iolC*, and *iolA* gene products (19) (Fig. 1). The *iolA* gene encodes the methylmalonate semialdehyde dehydrogenase, which oxidizes both methylmalonate semialdehyde and malonate semialdehyde, and therefore, *iolA* has been renamed *mmsA* in *B. subtilis* (http://genolist.pasteur.fr/SubtiList).

Our previous work indicated that the *iolR* gene product is involved in the regulation of the structural inositol catabolic genes. The *myo*- as well as the *scyllo*-inositol dehydrogenase activities were highly upregulated in an *S. meliloti* IolR mutant, even under noninducing conditions (19). Also, plasmid-borne gene fusions to the *idhA* and *iolC* genes were no longer repressed in an *iolR* mutant of *Rhizobium leguminosarum* bv. viciae (16). The deduced IolR protein belongs to the RpiR-like transcriptional regulator family and contains a predicted DNA-binding helix-turn-helix motif at its N terminus and a predicted phosphosugar-binding site at its C terminus. Conserved putative IolR-binding motifs were identified in the regions upstream of the *S. meliloti idhA*, *iolY*, *iolR*, and *iolC* genes (4, 19). These findings, together with our result that *iolR* mutants cannot compete with the wild type for nodule occupancy

* Corresponding author. Mailing address: Department of Biological Sciences, Western Michigan University, Kalamazoo, MI 49008-5410. Phone: (269) 387-5868. Fax: (269) 387-5609. E-mail: Silvia.Rossbach@wmich.edu.

† Supplemental material for this article may be found at http://jb.asm.org/.

▽ Published ahead of print on 22 July 2011.

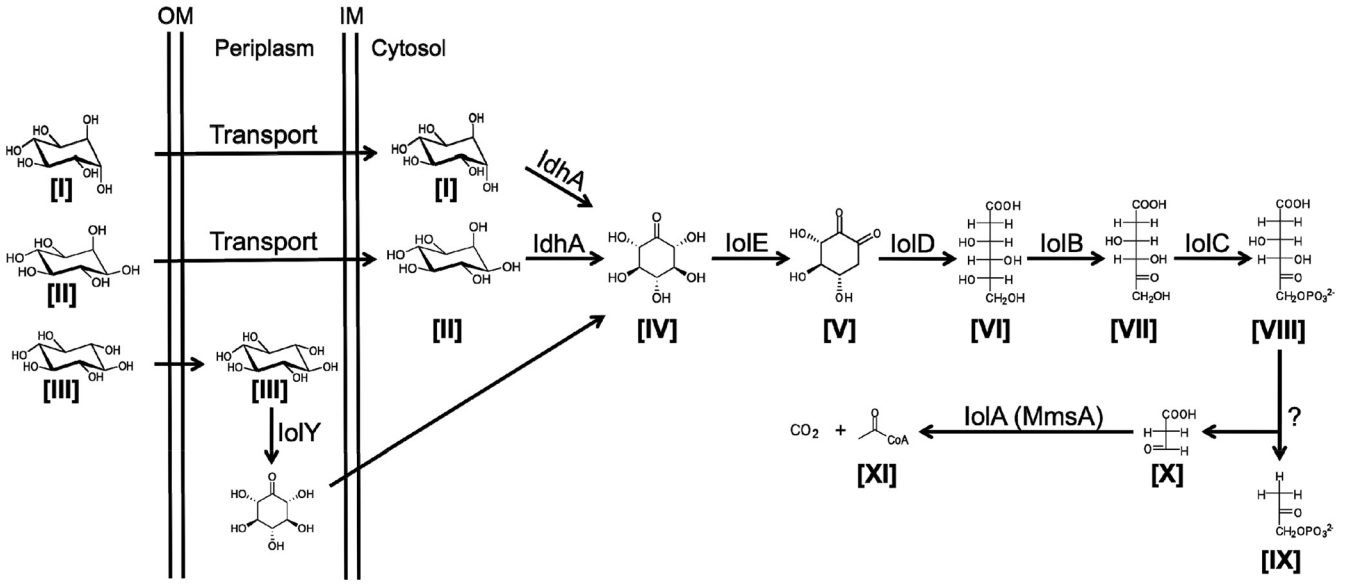


FIG. 1. Suggested inositol catabolic pathway in *S. meliloti*. Compounds: [I], D-*chiro*-inositol; [II], *myo*-inositol; [III], *scyllo*-inositol; [IV], 2-keto-*myo*-inositol; [V], 3-D-(3,4/5)-trihydroxycyclohexane-1,2-dione; [VI], 5-deoxy glucuronic acid; [VII] 2-deoxy-5-keto-D-gluconic acid; [VIII] 2-deoxy-5-keto-D-gluconic acid 6-phosphate; [IX] dihydroxyacetone phosphate; [X], malonate semialdehyde (MSA); [XI], acetyl coenzyme A. Enzymes: IdhA, *myo*-inositol dehydrogenase; IolY, *scyllo*-inositol dehydrogenase; IolE, 2KMI dehydratase; IolD, 3-D-(3,5/4)-trihydroxycyclohexane-1,2-dione hydrolase; IolB, 5-deoxy-glucuronate isomerase; IolC, 2-deoxy-5-keto-D-gluconic acid kinase; IolA (MmsA), methylmalonate semialdehyde dehydrogenase.

(19), prompted us to intensify our studies analyzing the role of IolR in *iol* gene expression.

Here, we report the transcriptional organization of the *iol* genes and their regulation through IolR on the basis of results from reverse transcriptase (RT) PCR and electrophoretic mobility shift assays (EMSAs). Gene expression studies and enzyme assays were used to elucidate the nature of the inducer of the *iol* genes. Moreover, a new role was found for the *S. meliloti iolA* gene in valine catabolism.

## MATERIALS AND METHODS

**Microbiological methods.** The bacterial strains and plasmids used in this study are listed in Table 1. *Escherichia coli* strains were grown at 37°C in Luria-Bertani (LB) medium (32). Antibiotics for *E. coli* were ampicillin (Ap; 100 μg/ml) and tetracycline (Tc; 10 μg/ml). *S. meliloti* cultures were grown at 28°C. Rich medium for *S. meliloti* was tryptone yeast (TY) medium (2); minimal media were minimal M medium (30) with 0.1% (vol/vol) $NH_4Cl$ as the sole nitrogen (N) source for the catabolism and enzyme assays or GTS minimal medium for the selection of exconjugants (18). Carbon (C) sources were added to the minimal media at a final concentration of 0.2% (vol/vol) unless otherwise indicated. Antibiotics for *S. meliloti* were streptomycin (Sm; 250 μg/ml), kanamycin (Km; 200 μg/ml), and Tc (10 μg/ml). For the catabolism study with valine, alanine, leucine, and isoleucine as sole C sources, *S. meliloti* precultures were inoculated 1:100 into liquid minimal M medium. Cultures were grown on a shaking incubator, and the growth was determined spectrophotometrically at 600 nm every 48 h for 10 days. Triparental conjugations were performed according to the methods described by Rossbach and de Bruijn (29).

**DNA manipulations.** Preparation of plasmid DNA, DNA digests, agarose gel electrophoresis, and cloning and transformation of *E. coli* cells were performed following established protocols (32).

**Expression of *iolR* and purification of IolR-His$_6$.** The *iolR* gene was PCR amplified from a liquid *S. meliloti* 2011 culture. Primers were engineered to contain an NdeI site at the 5′ end and an EcoRI site at the 3′ end, not including the stop codon of *iolR* (see Table S1 in the supplemental material). The purified PCR product was cloned into the expression vector pET21a (Table 1), creating a C-terminal His tag fusion. DNA sequencing confirmed the correct sequence of the *iolR* fusion (Cornell, Life Sciences Core Laboratory Center, Ithaca, NY). *E. coli* BL21 Star(DE3) (Invitrogen, Carlsbad, CA) containing the resulting plasmid, pPK64 (Table 1), was cultured in 5 ml LB (Ap) overnight and inoculated 1:100 in a 250-ml flask containing 50 ml LB medium (Ap) and grown to an optical density at 600 nm ($OD_{600}$) of 0.6. Expression of *iolR* was induced with 0.4 mM isopropyl-β-D-thiogalactopyranoside (IPTG). After 4 h of incubation, the cells were harvested via centrifugation at 5,000 × *g* and resuspended in 4 ml EW buffer (50 mM sodium phosphate, pH 7, 300 mM NaCl). The cells were sonicated at 50 W with three 30-s periods (XL-2020 sonicator; Misonix, Farmingdale, NY), and a cell extract was prepared by centrifugation at 20,000 × *g* for 30 min at 4°C. A cobalt-based TALONspin column (Clontech Laboratories, Mountain View, CA) was equilibrated with 5 ml EW buffer. The cell extract was applied to the column three times using gravity flow. The resin was washed with 5 ml of EW Buffer. IolR-His$_6$ was eluted with 150 mM imidazole in EW buffer, and four fractions were collected. The total protein concentrations of the eluted fractions were determined with a Coomassie Plus protein assay kit (Pierce Biotechnology, Rockford, IL). The purity of the overexpressed IolR-His$_6$ was verified via SDS-PAGE and Coomassie staining (see Fig. S1 in the supplemental material).

**EMSA.** PCR fragments that contained the putative promoter sequences of the *idhA*, *iolY*, *iolR*, *iolC*, and *iolA* genes as well as the known promoter of the *nodD1* gene were PCR amplified from a liquid *S. meliloti* 2011 culture. The PCR fragments with sizes of between 90 and 108 bp were used as substrates in the EMSA. Ten nanograms of DNA was mixed with increasing concentrations of IolR-His$_6$ (0 to 0.5 μM) in binding buffer (25 mM HEPES, pH 7.5, 5 mM sodium acetate, 5 mM $MgCl_2$, 0.1 mM EDTA, 1 mM dithiothreitol, 200 ng/ml bovine serum albumin, and 10% glycerol) in a total volume of 10 μl, and the mixture was incubated at 16°C for 1 h. The samples were loaded with 2 μl 6× loading buffer (3× Tris borate-EDTA buffer [pH 8]), 18% glycerol, 0.3% xylene cyanol, 0.03% bromphenol blue) on a native 5% polyacrylamide (PAA) gel. Initially, 80 V for 15 min was applied with ice-cold 0.5× Tris-borate-EDTA buffer at room temperature, followed by 25 V for 6 h at 4°C. PAA gels were stained with ethidium bromide and visualized by UV.

**RT-PCR of the *idhA*, *iolYRCDEB*, and *iolA* genes.** *S. meliloti* 2011 TY medium precultures were diluted 1:100 in 5 ml minimal M medium with 0.2% glycerol or *myo*-inositol as the sole C source. Five hundred microliters of mid-exponential-phase cultures ($OD_{600}$ = 0.5) was harvested via centrifugation at 4,500 × *g* for 10 min. Extraction of total RNA was performed using a Quick-RNA MiniPrep kit (Zymo, Irvine, CA) according to the manufacturer's instructions. One microliter of the total RNA served as template in reverse transcriptase PCR using a One-Step RT-PCR kit (Qiagen, Valencia, CA) according to the manufacturer's

TABLE 1. Bacterial strains and plasmids

| Strain or plasmid | Relevant characteristics or phenotype | Reference or source |
|---|---|---|
| Strains | | |
| *Escherichia coli* | | |
| DH5α | *supE44* Δ*lacU169* (ϕ80*lacZ*ΔM15) *hsdR17 recA1 endA1 gyrA96 thi-1 relA1* | 32 |
| BL21 Star(DE3) | $F^-$ *ompT hsdS*$_B$($r_B^-$ $m_B^-$) *gal dcm rne-131* (DE3) | Invitrogen |
| *Sinorhizobium meliloti* | | |
| 1021 | Wild-type, $Sm^r$ derivative of SU47 | 23 |
| 2011 | Wild-type, $Sm^r$ derivative of SU47 | 24 |
| TIOLB | 1021 *smc00432*::pVO155 $Sm^r$ $Km^r$ | 19 |
| WIDHA | 2011mTn*5*-STM.5.11.A04 *smb20899*::*gus* $Sm^r$ $Km^r$ | 27 |
| WIOLR | 2011mTn*5*-STM.4.13.C12 *smc01164*::*gus* $Sm^r$ $Km^r$ | 27 |
| WIOLC | 2011mTn*5*-STM.1.11.A02 *smc01165*::*gus* $Sm^r$ $Km^r$ | 27 |
| WIOLD | 2011mTn*5*-STM.1.13.D10 *smc01166*::*gus* $Sm^r$ $Km^r$ | 27 |
| WIOLE | 2011mTn*5*-STM.1.01.B03 *smc00433*::*gus* $Sm^r$ $Km^r$ | 27 |
| WMMSA | 2011mTn*5*-STM.4.03.B06 *smc00781*::*gus* $Sm^r$ $Km^r$ | 27 |
| Plasmids | | |
| pRK2013 | *mob tra* $Km^r$ | 10 |
| pET21a(+) | Protein expression vector, $Ap^r$ | Invitrogen |
| pPK64 | pET21a containing 857-bp fragment of *iolR* | This study |
| pTE3 | Broad-host-range expression vector, $Tc^r$ | 8 |
| pIOLR | pTE3 containing 991-bp fragment of *iolR* | This study |
| pIOLC | pTE3 containing 2,412-bp fragment of *iolC* | 19 |
| pIOLD | pTE3 containing 2,776-bp fragment of *iolD* | 19 |
| pIOLE | pTE3 containing 945-bp fragment of *iolE* | 19 |
| pIOLB | pTE3 containing 881-bp fragment of *iolB* | 19 |

instructions. The primers used (see Table S1 in the supplemental material) flank each of the intergenic regions in the *iolYRCDEB* gene cluster or are homologous to the intragenic regions of the *idhA* and *iolA* genes. The cytochrome *c* oxidase gene (*smc01981*) served as a control. To ensure that the RNA was DNA free, a control PCR with the RNA as the template was conducted. Initial generation of cDNA was performed at 55°C for 30 min. Heat inactivation of RT and activation of the *Taq* polymerase were accomplished by heating at 95°C for 15 min. Amplification of cDNA was carried out in 30 cycles of denaturation at 94°C for 1 min, primer annealing at 59°C for 1 min, and primer extension at 72°C for 1.5 min, followed by a final elongation step at 72°C for 10 min. The PCR products were separated by electrophoresis on a 1% agarose gel.

**Complementation of *S. meliloti* 2011 *iolR* mutant.** A DNA fragment containing the *iolR* gene, including its ribosomal binding site, was PCR amplified from a liquid *S. meliloti* culture with primers engineered to contain a NsiI site at the 5′ end and a BglII site at the 3′ end (see Table S1 in the supplemental material). The PCR product was cloned into the broad-host-range expression vector pTE3 (Table 1) under the control of the *Salmonella trp* promoter, which is constitutively expressed in *S. meliloti* (8). The resulting plasmid, pIOLR (Table 1), and pTE3 as an empty-vector control were introduced into the *S. meliloti iolR* mutant via triparental mating. The presence of the wild type and of the mutated *iolR* gene was confirmed via PCR.

**β-Glucuronidase assays.** The β-glucuronidase assays were carried out as described previously (19). Briefly, precultures of *S. meliloti* strains were diluted 1:100 in 5 ml minimal M medium containing *myo*-inositol, glycerol, glucose, succinate, or combinations thereof as the sole C source (final concentration, 0.2%). The reaction rate was expressed in nmol *p*-nitrophenol produced $min^{-1}$ $OD_{600}$ $unit^{-1}$ ± standard error of the mean (SEM). The values represent the mean of two independent experiments, and each assay was carried out in duplicate. As a control, the wild-type strain did not exhibit any detectable β-glucuronidase activity due to the absence of the *gusA* gene.

**NAD(H)-dependent *myo*-inositol dehydrogenase assays.** NAD(H)-dependent *myo*-inositol dehydrogenase assays were conducted as described previously (19). Briefly, *S. meliloti* precultures were diluted 1:100 into 500-ml Erlenmeyer flasks containing 100 ml minimal M medium with 0.1% $NH_4Cl$ as the N source and 0.2% glycerol or *myo*-inositol as the C source. The specific *myo*-inositol dehydrogenase activity was expressed as nmol $NAD^+$ reduced $min^{-1}$ mg of $protein^{-1}$ ± SEM. The values represent the mean of two independent experiments, each of them performed in duplicate.

## RESULTS

**IolR binds upstream of the *idhA*, *iolY*, *iolR*, and *iolC* genes.** The *S. meliloti iolR* gene encodes a protein of 284 amino acids. It displays a DNA-binding domain with a helix-turn-helix (HTH) motif at its N terminus (residues 19 to 88; PFAM 01418), followed by a predicted C-terminal sugar isomerase (SIS) domain (residues 146 to 271; PFAM 01380). To verify the DNA-binding properties of IolR, the *iolR* gene was cloned in the pET21a vector and expressed in *E. coli*, and IolR-$His_6$ was purified from the soluble fraction. The purified recombinant IolR-$His_6$ had an apparent molecular mass of 32 kDa on SDS-PAGE (see Fig. S2 in the supplemental material), which correlates well with its calculated molecular mass (31.99 kDa).

The upstream regions of the *idhA*, *iolY*, *iolR*, and *iolC* genes each contain variations of a putative IolR-binding motif (5′-G GAA-$N_6$-TTCC-3′) (Fig. 2B). We conducted an electrophoretic mobility shift assay to investigate the IolR-DNA interactions *in vitro*. Increasing concentrations of the purified IolR-$His_6$ protein (0 to 0.5 μM) were added to 10 ng of eight individual DNA fragments. Five different fragments represented the upstream regions of the *idhA*, *iolY*, *iolR*, *iolC*, and *iolA* genes. DNA shifts were observed for the *idhA*, *iolY*, *iolR*, and *iolC* fragments (Fig. 2A). Retardation of the fragments was achieved by IolR concentrations as low as 0.03 μM and increased with increasing protein concentration (Fig. 2A). The upstream region of *iolA* lacks the predicted IolR-binding motif, and no DNA shift was visible, indicating that the *iolA* gene is regulated independently of IolR (Fig. 2A). The promoter region of the *nodD1* gene served as an IolR-independent negative control, and no DNA retardation occurred, as expected

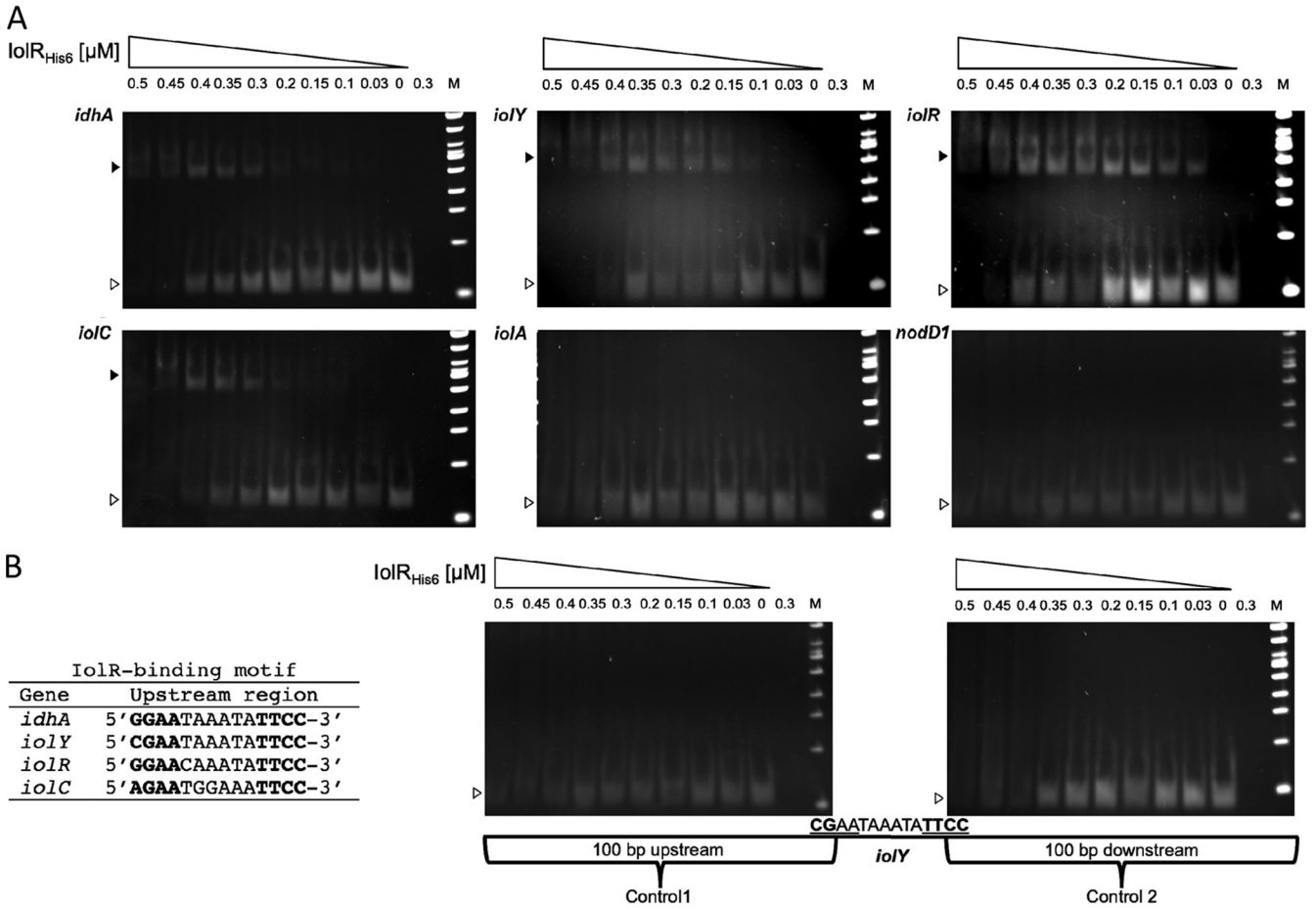


FIG. 2. IolR-DNA-binding assay. Increasing concentrations of purified IolR-His$_6$ protein (indicated at the top of each lane) were incubated with 10 ng of 8 different PCR products. The positions of free DNA (open arrowheads) and IolR-DNA complexes (solid arrowheads) are indicated. As a control, 0.3 μM protein without DNA in binding buffer was loaded. (A) EMSA with the upstream regions of *idhA*, *iolY*, *iolR*, *iolC*, *iolA*, and *nodD1* (IolR-independent control). (B) The identified IolR-binding motifs of the *idhA*, *iolY*, *iolR*, and *iolC* genes; controls 1 and 2, DNA fragments containing the sequences up- and downstream of the IolR-binding motif of *iolY*, respectively; lanes M, 100-bp ladder.

(Fig. 2A). Two additional control fragments were included to verify the requirement of the putative IolR-binding site for the IolR-DNA interaction. Control fragment 1 contained the DNA sequence of the *iolY* regulatory region upstream of the predicted IolR-binding motif, including the first 2 bases of the motif, while control fragment 2 contained the sequence downstream of the predicted motif, including its last two bases. No DNA retardation was visible for controls 1 and 2 (Fig. 2B). Thus, IolR did not bind to the sequences flanking the predicted binding motif in the putative *iolY* promoter, confirming the requirement of the conserved consensus sequence for IolR binding.

**Transcriptional organization of *iol* genes.** An operon prediction program (www.microbesonline.org) suggests that the *idhA*, *iolA*, *iolY*, and *iolR* genes are monocistronically transcribed, whereas *iolCDEB* comprise an operon. This prediction is supported by the finding that IolR binds to the upstream regions of *idhA*, *iolY*, *iolR*, and *iolC* (Fig. 2A). To elucidate the *iol* operon structure, reverse transcriptase PCR was performed using the total RNA isolated from *S. meliloti* 2011 grown in minimal medium containing *myo*-inositol or glycerol as the sole C source. cDNA was successfully amplified from all five intergenic regions of the *iolYRCDEB* cluster, confirming that these genes are transcribed as one single mRNA (Fig. 3). Quantitative differences were found in the amount of the amplified cDNA. In all instances, the PCR fragments showed greater intensity when they were amplified from the RNA of cells grown with *myo*-inositol than from cells grown with glycerol as the sole C source. Thus, we conclude that the *iolYRCDEB* operon is expressed at low levels when *S. meliloti* is grown on glycerol, but it is expressed at higher levels when cells are grown with *myo*-inositol (Fig. 3). We also conducted RT-PCR to investigate the expression of the separately located *idhA* and *iolA* genes. The cDNA was amplified from the intragenic regions of both genes when grown on glycerol, and their expression increased, too, when grown with *myo*-inositol (Fig. 3). The *smc01981* gene, encoding a putative cytochrome *c* oxidase, served as a control. The amount of cDNA produced from its intragenic region was the same, regardless of whether *S. meliloti* was grown with glycerol or *myo*-inositol (Fig. 3). The size of the cDNA fragments corresponded to the size of the fragments obtained from the *S. meliloti* genomic DNA (be-

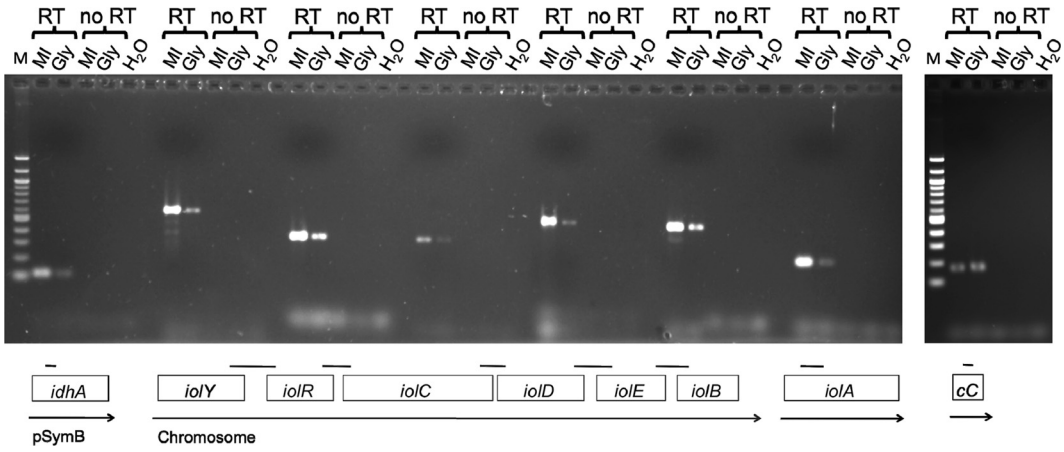


FIG. 3. Transcriptional organization of *S. meliloti* inositol catabolic genes. The 2011 wild-type strain was grown in minimal medium with *myo*-inositol (MI) or glycerol (Gly) as the sole carbon source. The total RNA was purified and used as a template in RT-PCR (RT). cDNA was amplified with primers flanking the indicated intergenic regions of the *iolYRCDEB* cluster and the intragenic regions of the *idhA*, *iolA*, and *smc01981* (cytochrome *c* [cC]) genes. Boxes represent the individual inositol genes, and arrows represent transcriptional units. As controls, PCR was performed with RNA samples (no RT) and no template ($H_2O$).

tween 106 and 627 bp; see Fig. S2 in the supplemental material). The isolated RNA was free of DNA, as no cDNA was produced in the no-RT control reactions (Fig. 3).

**Regulation of *iol* gene expression.** The *iolR*, *iolD*, and *iolE* mutants of *S. meliloti* 2011 contain mTn*5*-STM::*gusA* insertions, obtained by transposon mini-Tn*5* signature-tagged mutagenesis (mTn*5*-STM), in the same orientation as the respective genes, creating transcriptional fusions that allow the investigation of *iolRDE* gene expression by determining the β-glucuronidase activity (27). (The mTn*5*-STM mutation in the *iolC* mutant is oriented in the opposite direction as the *iolC* gene, and no transposon-induced *iolB* mutant is available in *S. meliloti* strain 2011.)

It was previously shown in growth studies that cloned fragments carrying the individual *iol* genes complemented the *iolC*, *iolD*, *iolE*, and *iolB* mutants (19). Here we used the same mutant strains and an *iolR* mutant expressing the corresponding *iol* genes from the constitutive promoter of the pTE3 vector (8) to study *iol* gene induction. The *iolR*, *iolD*, and *iolE* mutants containing the empty pTE3 vector served as controls. All strains were grown in minimal medium with glycerol or *myo*-inositol as the sole C source. The WIOLR/pTE3 mutant displayed high β-glucuronidase activities under both growth conditions (Fig. 4). The *iolR* gene was induced to similar levels in the complemented WIOLR/pIOLR strain in the presence of *myo*-inositol, but when grown with glycerol, *iolR* was only minimally expressed (Fig. 4), indicating that a functional *iolR* gene is necessary for the repression of its own gene.

The WIOLD/pTE3 and WIOLE/pTE3 mutants displayed very low β-glucuronidase activities regardless of whether they were grown with glycerol or *myo*-inositol. Nevertheless, *iolD* and *iolE* gene expression was induced in the complemented WIOLD/pIOLD and WIOLE/pIOLE mutants when grown with *myo*-inositol but not with glycerol (Fig. 4). This shows that functional *iolD* and *iolE* genes are required for inducer production, supporting the notion that not *myo*-inositol itself but a later pathway intermediate functions as the inducer of the *iol* genes in *S. meliloti*.

**Regulation of *myo*-inositol dehydrogenase activity.** To identify the metabolic step that produces the inducer of the *iol* genes, we carried out *myo*-inositol dehydrogenase assays with the *S. meliloti* wild type and the complemented *iol* mutant strains. The specific *myo*-inositol dehydrogenase activities of the wild-type strains 2011 and 1021, carrying the empty pTE3 vector as a control, were low when grown with glycerol as the sole C source (11 and 2 nmol $min^{-1}$ mg of $protein^{-1}$, respectively; Fig. 5). When grown with *myo*-inositol, the wild-type strains displayed *myo*-inositol dehydrogenase activities of 142 and 169 nmol $min^{-1}$ mg of $protein^{-1}$, respectively (Fig. 5). The WIOLR/pTE3 strain displayed a 4- to 5-fold higher *myo*-ino-

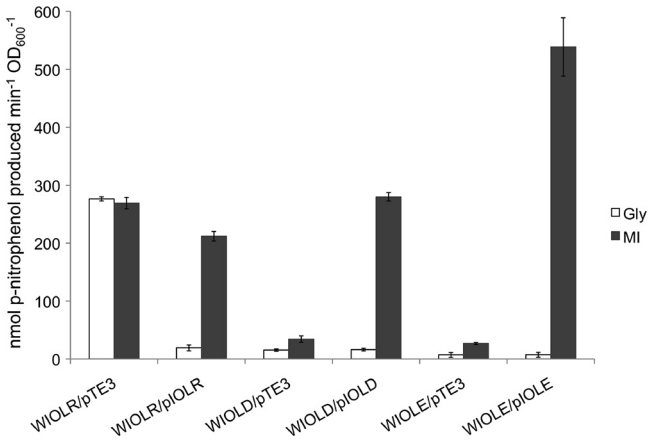


FIG. 4. β-Glucuronidase activities of the *S. meliloti iolR*-, *iolD*-, and *iolE-gusA* reporter gene fusions in the respective mutant strains. The WIOLR/pTE3, WIOLD/pTE3, and WIOLE/pTE3 strains harbor the empty vector pTE3 as a control, while the WIOLR/pIOLR, WIOLD/pIOLD, and WIOLE/pIOLE strains express the corresponding wild-type genes from pTE3. The reaction rate is expressed in nmol *p*-nitrophenol produced per minute per $OD_{600}$ unit. Bars represent the average of two independent experiments, and error bars denote ±SEM. Cultures were grown in minimal medium containing glycerol (Gly) or *myo*-inositol (MI) as the sole carbon source.

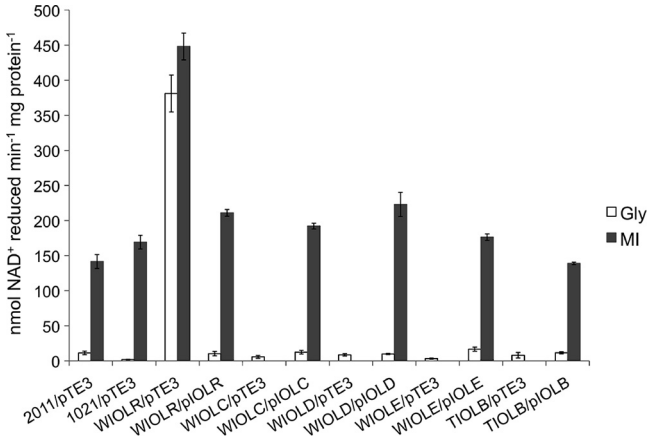


FIG. 5. NAD(H)-dependent *myo*-inositol dehydrogenase assay with crude cell extracts obtained from *S. meliloti* wild-type and mutant strains grown in minimal medium containing 0.2% glycerol (Gly) or *myo*-inositol (MI) as the sole carbon source. The reaction rate is expressed in nmol $NAD^+$ reduced per minute per mg protein. Bars represent the average of two independent experiments, and error bars denote ±SEM. The WIOLC/pTE3, WIOLD/pTE3, WIOLE/pTE3, and TIOLB/pTE3 strains did not grow in minimal medium with *myo*-inositol as the sole carbon source.

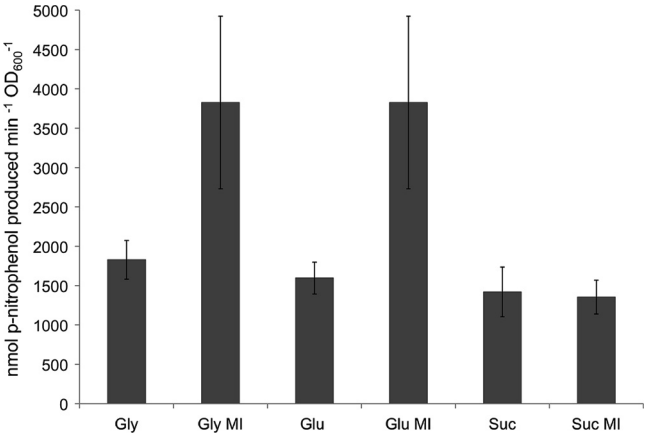


FIG. 6. β-Glucuronidase activities of the *S. meliloti iolA-gusA* reporter gene fusion in the *iolA* mutant strain. The WIOLA mutant was grown in minimal medium containing *myo*-inositol (MI), glycerol (Gly), glucose (Glu), succinate (Suc), or combinations thereof at a final concentration of 0.2% as the carbon source. Bars represent the average of two independent experiments, and error bars denote ±SEM.

sitol dehydrogenase activity than the wild type, even when grown without *myo*-inositol (Fig. 5). The *myo*-inositol dehydrogenase activity of the complemented WIOLR/pIolR strain was comparable to wild-type activity on both carbon sources (Fig. 5). The WIOLC/pTE3, WIOLD/pTE3, WIOLE/pTE3, and TIOLB/pTE3 strains exhibited very low *myo*-dehydrogenase activities when grown with glycerol (Fig. 5). These strains do not grow with *myo*-inositol as the sole C source; therefore, enzyme activities could not be determined. Previously, *myo*-inositol dehydrogenase activities were not detectable in the individual *iolCDEB* mutants even when grown with *myo*-inositol as an additional source (19). The *myo*-inositol dehydrogenase activities were low in the WIOLC/pIOLC, WIOLD/pIOLD, WIOLE/pIOLE, and TIOLB/pIOLB mutants when grown with glycerol as the sole C source. The complemented strains, however, displayed *myo*-inositol dehydrogenase activities comparable to the wild-type activity when grown with *myo*-inositol (Fig. 5). The *iolA* mutant is affected in the final step of the proposed inositol catabolic pathway (Fig. 1). Interestingly, the *myo*-inositol dehydrogenase activity of this mutant was almost 2-fold higher than the wild-type activities (268 nmol $min^{-1}$ mg of $protein^{-1}$). The higher activity could be due to inducer accumulation in the *iolA* mutant strain. These findings allow the conclusion that the *iolCDEB* gene products, but not the *iolA* gene product, are required for the production of the inducer.

**The *iolA* gene is constitutively expressed.** The *iolA* mutant contains a transcriptional *gusA* fusion in the same orientation as *iolA*, allowing the investigation of *iolA* expression (27). Since the *iolA* gene is required for the growth with inositol, the respective mutant cannot grow if inositol is offered as the only C source (4, 19). Therefore, the *iolA* mutant was grown in minimal medium with either glycerol, glucose, or succinate as the sole C source or in combination with *myo*-inositol for the analysis of gene expression with the β-glucuronidase assay (Fig. 6). The *iolA-gusA* fusion was constitutively expressed at high levels in the corresponding mutant, and the expression increased approximately 2-fold in the presence of *myo*-inositol when grown with glycerol or glucose but remained the same when grown with succinate and *myo*-inositol (Fig. 6). In general, the *iolA-gusA* fusion was expressed at much higher levels than the *iolR*, *iolD*, and *iolE* fusions (compare Fig. 5 and 6).

**The *iolA* gene is required for valine catabolism.** The finding that the *iolA* gene is constitutively expressed and not coregulated with the other *iol* genes indicates that its gene product is not part of the core inositol catabolic pathway but might play a more general role in the metabolism of *S. meliloti*. The *iolA*-encoded methylmalonate semialdehyde dehydrogenase (MmsA) is known to be required for valine metabolism in *Pseudomonas* spp. and *Streptomyces coelicolor* (1, 28, 34, 43) Therefore, a possible role of IolA in valine metabolism of *S. meliloti* was investigated by conducting a growth study in minimal medium with 0.2% valine as the sole C source. The *iolA* mutant did not grow with valine as the sole C source, whereas the wild type reached an $OD_{600}$ of 1.3 after 10 days (Fig. 7). As a control, the amino acids alanine, leucine, and isoleucine were offered as sole C sources. When grown with these amino acids, *iolA* mutant growth was comparable to that of the wild type (data not shown).

## DISCUSSION

The transcriptional repressors of the inositol catabolic pathways in *Firmicutes* and Gram-negative bacteria belong to different families of regulatory proteins, although all are designated IolR on the basis of their function. The *iolR* gene products in *Firmicutes* belong to the DeoR family, while the IolR proteins in Gram-negative bacteria, including *S. meliloti*, are RpiR-like transcriptional regulators (4, 17, 39, 42). The deduced IolR protein sequence contains a helix-turn-helix motif at its N terminus, followed by a SIS domain that is predicted to bind phosphosugars. Members of the RpiR family have been shown to function as positive and negative transcriptional

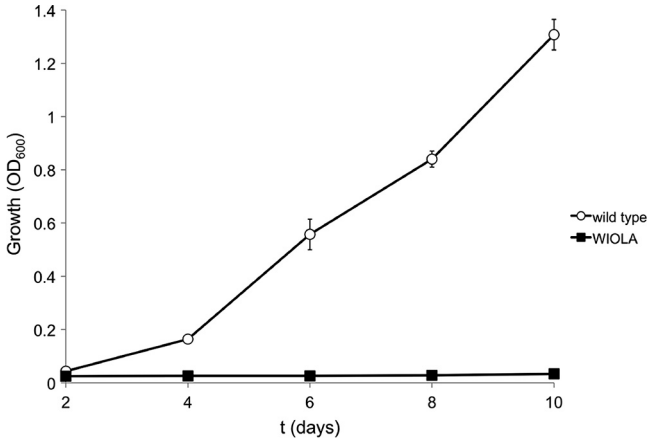


FIG. 7. Growth of *S. meliloti* wild-type strain 2011 (open circles) and the corresponding *iolA* mutant (solid squares) with 0.2% valine as the sole carbon source in minimal medium. The optical density was determined spectrophotometrically at 600 nm. Bars represent the average of two experiments, and error bars denote ±SEM.

regulators. In *B. subtilis*, maltose metabolism is regulated by an RpiR-like transcriptional activator (38), whereas RpiR-like repressors control ribose and *N*-acetylmuramic acid catabolism in *Escherichia coli* and glucose metabolism in *Pseudomonas putida* (6, 14, 33). The inositol catabolism genes in *Caulobacter crescentus* and *Salmonella enterica* are also regulated by RpiR-like IolR repressors (4, 20).

**A conserved IolR-binding motif is required for IolR-DNA interactions.** The purified IolR-$His_6$ bound to the regulatory sequences of the *idhA*, *iolY*, *iolR*, and *iolC* genes, which contain variations of the conserved IolR-binding motif 5′-GGAA-$N_6$-TTCC-3′ (Fig. 2B), but IolR-$His_6$ did not interact with the upstream region of *iolA*, which lacks the motif (Fig. 2A). Also, IolR did not bind to the fragments containing the sequences directly up- and downstream of the conserved motif of the *iolY* gene, indicating that this motif is required for the IolR-DNA interactions (Fig. 2B).

**Induction of inositol catabolism.** IolR did not completely repress *idhA* and *iolYRCDEB* expression in the absence of inositol. The reverse transcriptase PCR revealed that the *iol* genes are weakly constitutively expressed (Fig. 3), suggesting that the inositol catabolic enzymes are always present in the cytoplasm at low concentrations. This is confirmed by the results of the *myo*-inositol dehydrogenase assays with an uninduced *S. meliloti* wild type and its corresponding *idhA* mutant. When grown with glucose or glycerol, the *myo*-inositol dehydrogenase activity of the wild-type cell extract was significantly higher than the activity of the *idhA* mutant (12, 19). The constant presence of the inositol catabolic enzymes is probably required for the production of the IolR-antagonizing effector (inducer). We have shown previously that *myo*-inositol dehydrogenase activities were absent in the *iolC*, *iolD*, *iolE*, and *iolB* mutants (19). Here, we demonstrated that the *iolC*, *iolD*, *iolE*, and *iolB* genes and their gene products are required for induction of *iol* gene expression, exemplified by the results of the β-glucuronidase and *myo*-inositol dehydrogenase assays with the complemented strains (Fig. 4 and 5). It is important to note that the *myo*-inositol dehydrogenase activity of the *iolA* mutant was 2-fold higher than that of the wild type. The *iolA* gene product, the methylmalonate semialdehyde dehydrogenase, is proposed to be the last enzyme of the inositol catabolic pathway (Fig. 1). The increased *myo*-inositol dehydrogenase activity of the *iolA* mutant supports the notion that the inducer of the *iol* genes is produced by the action of IolCDEB. The increased *myo*-inositol dehydrogenase activity in the *iolA* mutant could be due to inducer accumulation.

The IolC reaction is the only step in the inositol pathway that yields a phosphosugar, 2-keto-5-deoxy-D-gluconic acid 6-phosphate (KDGP), which is likely to interact with the phosphosugar-binding domain (SIS) of IolR. Thus, we suggest that it is KDPG that functions as the IolR-antagonizing effector (inducer). KDGP has also been identified to be the inducer of inositol catabolism in *B. subtilis* (41). It is interesting to note that the Entner-Doudoroff pathway intermediate, 2-keto-3-deoxy-D-gluconic acid 6-phosphate, a structurally similar phosphosugar, binds to the RpiR-like HexR repressor and induces glucose metabolism in *P. putida* (6).

***S. meliloti iol* gene regulation is fine-tuned.** The occurrence of three regulatory regions in the *iolYRCDEB* operon suggests that the operon is under the control of the single predicted promoter upstream of *iolY* but also contains two additional repressor-binding sites. It is not uncommon to have multiple repressor-binding sites in one operon. For example, three operators have been identified in the prototypical *E. coli lac* operon, in which DNA looping is a feature of regulation by the Lac repressor (26, 31). Interestingly, the sequences of the conserved IolR-binding motifs in the *iolYRCDEB* operon differ slightly from one another (Fig. 2B). The first base of the motif in the regulatory region of *iolR* is a guanine (5′-GGAA-$N_6$-TTCC-3′), which agrees with the predicted consensus sequence. The first base of the motif in p*iolY* is a cytosine (5′-CGAA-$N_6$-TTCC-3′), and the first base in the *iolC* motif is an adenine (5′-AGAA-$N_6$-TTCC-3′). The last two motifs are imperfect palindromes, which could result in different IolR-binding affinities.

The structure of $\sigma^{70}$-dependent promoters in *S. meliloti* has been elucidated to be 5′-CTTGAC-$N_{17}$-CTATAT-3′ (22). The −35 region is fairly well conserved and can start with a C, a G, or an A, while the −10 region is poorly conserved and diverse (22). We screened the upstream sequences of the IolR-dependent *idhA* and *iolYRCDEB* genes for known promoter structures in *S. meliloti.* No obvious promoter sequences were found upstream of the *iolR* and *iolC* genes. Nevertheless, the upstream region of the *idhA* and *iolY* genes contains possible −35 and −10 regions of $\sigma^{70}$-dependent promoters, 5′-CTTGAC-$N_{17}$-AATAAA-3′ and 5′-ATTGAC-$N_{17}$-TTTCAT-3′, respectively. The IolR-binding motif upstream of the *idhA* gene overlaps with the predicted −10 region of p*idhA*, while the IolR-binding element of p*iolY* is located directly upstream of the −35 region (see Fig. S3 in the supplemental material).

**The *iolA* gene product is not part of the core inositol catabolic pathway.** The *iolA* gene encodes a methylmalonate semialdehyde dehydrogenase, the last enzyme in the proposed inositol catabolic pathway, and was shown to be required for the catabolism of *myo*-, *scyllo*-, and D-*chiro*-inositol in *S. meliloti* (4, 19). The expression of *iolA* is IolR dependent in *B. subtilis* and *S. enterica* (20, 41). This is different in *S. meliloti*, since we found that the *iolA* gene is constitutively expressed in the

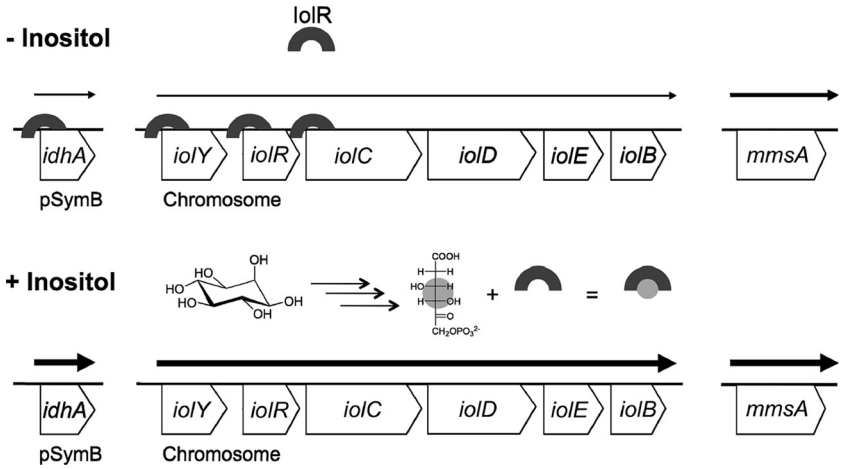


FIG. 8. Model for IolR-mediated *iol* gene regulation. IolR binds to the conserved binding motif $GGAAN_6TTCC$ in the regulatory region of the *idhA* gene and in the three regulatory regions of the *iolYRCDEB* operon in the absence of inositol, but it does not repress transcription completely. Inositol is being catabolized as soon as it is imported into the cell, and the late pathway intermediate, 2-deoxy-5-keto-D-gluconic acid 6-phosphate, antagonizes the IolR-mediated transcriptional repression. The *mmsA* (*iolA*) gene is constitutively expressed and is not subject to IolR regulation, but *mmsA* expression is nevertheless increased in the presence of inositol.

corresponding mutant, expressed at higher levels than the other inositol catabolism genes, and is subject to catabolite repression by succinate (Fig. 6). In contrast, succinate did not affect the expression of the other *iol* genes (19). Most importantly, the *iolA* promoter does not contain an IolR-binding motif, and no DNA retardation was visible in our experiments.

These results, together with the finding that *iolA* is required for valine catabolism, support the notion that in *S. meliloti* the methylmalonate semialdehyde dehydrogenase is not part of the core inositol catabolic pathway comprising the *idhA*, *iolY*, and *iolCDEB* gene products but has a more central metabolic role. Thus, we suggest annotating *iolA* as *mmsA*, as has been done in *B. subtilis* (http://genolist.pasteur.fr/SubtiList).

**Model for *iol* gene regulation and additional layers of control.** Our current model of the IolR-mediated regulation of the *S. meliloti iol* genes is summarized in Fig. 8. Since inositol compounds are common in legume plants and in the rhizosphere, they represent easily accessible carbon sources for *S. meliloti* (7, 19, 35, 37). Upon entering the cell, *myo*-, D-*chiro*-, and *scyllo*-inositols are catabolized and converted into the common pathway intermediate KDGP, which either is further metabolized (Fig. 1) or binds the IolR repressor and releases it from its target promoters and operators, including its own regulatory region. Weak, constitutive expression of the *iol* genes is required to maintain a small amount of the Iol proteins in the cell. This guarantees the downregulation of *iol* gene expression through IolR but also allows *S. meliloti* to quickly respond to the presence of various inositol compounds.

Since the *mmsA* gene showed a higher expression in the presence of inositol but is regulated independently of IolR, we conclude that additional regulatory mechanisms that modulate the expression of *mmsA* and possibly of the other *iol* genes must be present. From other work it is known that the *S. meliloti iol* genes are coregulated with signaling pathways important for the establishment of the nitrogen-fixing symbiosis. For example, the IdhA protein was found to accumulate in response to the activation by the SinI/ExpR quorum-sensing system, which contributes to the efficiency of nodule initiation (13). In addition, the transcription of the *iolY* and the *iolCDEB* genes was found to be positively regulated by the ExoS/ChvI two-component system, which is required for symbiotic development (5). Interestingly, not only the mutants with insertions in the structural inositol catabolic genes but also the *iolR* mutant were outcompeted by the *S. meliloti* wild type in a cochallenge experiment for nodule occupancy, highlighting the importance of accurate regulation of inositol catabolism (19).

The *iolR* and the other *iol* genes are well conserved among the *Alphaproteobacteria*, including the symbiotic nitrogen-fixing genera *Sinorhizobium*, *Mesorhizobium*, and *Rhizobium*, as well as plant- and animal-pathogenic species of *Agrobacterium* and *Brucella* (4). In *Brucella abortus*, an *iolE* homolog (previously *mocC*) was found to be required for the survival inside macrophages (9). Thus, the notion that inositols are involved in the microbial ecology of bacterium-host interactions pertains not only to nitrogen-fixing symbioses but also to pathogenic microbe-host associations.

## ACKNOWLEDGMENTS

We thank Anke Becker for providing the *S. meliloti* 2011 mTn*5*-STM mutants.

This work was supported in part by a dissertation completion and a Gwen Frostic Doctoral Fellowship from the Western Michigan University Graduate College, as well as a Faculty Research and Creative Activities Award from Western Michigan University.

## REFERENCES

1. **Bannerjee, D., L. E. Sanders, and J. R. Sokatch.** 1970. Properties of purified methylmalonate semialdehyde dehydrogenase of *Pseudomonas aeruginosa*. J. Biol. Chem. **245:**1828–1835.
2. **Beringer, J. E.** 1974. R factor transfer in *Rhizobium leguminosarum*. J. Gen. Microbiol. **84:**188–198.
3. **Berman, T., and B. Magasanik.** 1966. The pathway of *myo*-inositol degradation in *Aerobacter aerogenes*: dehydrogenation and dehydratation. J. Biol. Chem. **241:**800–806.
4. **Boutte, C. C., et al.** 2008. Genetic and computational identification of a conserved bacterial metabolic module. PLoS Genet. **4:**e1000310.
5. **Chen, E. J., R. F. Fisher, V. M. Perovich, E. A. Sabio, and S. R. Long.** 2009. Identification of direct transcriptional target genes of ExoS/ChvI two-component signaling in *Sinorhizobium meliloti*. J. Bacteriol. **191:**6833–6842.

6. **Daddaoua, A., T. Krell, and J. L. Ramos.** 2009. Regulation of glucose metabolism in *Pseudomonas:* the phosphorylative branch and Entner-Doudoroff enzymes are regulated by a repressor containing a sugar isomerase domain. J. Biol. Chem. **284:**21360–21368.
7. **Duke, J.** 1992. Handbook of phytochemical constituents of GRAS herbs and other economic plants. CRC Press, Inc., Boca Raton, FL.
8. **Egelhoff, T. T., and S. R. Long.** 1985. *Rhizobium meliloti* nodulation genes: identification of *nodDABC* gene products, purification of *nodA* protein, and expression of *nodA* in *Rhizobium meliloti*. J. Bacteriol. **164:**591–599.
9. **Eskra, L., A. Canavessi, M. Carey, and G. Splitter.** 2001. *Brucella abortus* genes identified following constitutive growth and macrophage infection. Infect. Immun. **69:**7736–7742.
10. **Figurski, D. H., and D. R. Helinski.** 1979. Replication of an origin-containing derivative of plasmid RK2 dependent on a plasmid function provided *in trans*. Proc. Natl. Acad. Sci. U. S. A. **76:**1648–1652.
11. **Fry, J., M. Wood, and P. S. Poole.** 2001. Investigation of *myo*-inositol catabolism in *Rhizobium leguminosarum* bv. viciae and its effect on nodulation competitiveness. Mol. Plant Microbe Interact. **14:**1016–1025.
12. **Galbraith, M. P., et al.** 1998. A functional *myo*-inositol catabolism pathway is essential for rhizopine utilization by *Sinorhizobium meliloti*. Microbiology **144:**2915–2924.
13. **Gao, M., et al.** 2005. *sinI*- and *expR*-dependent quorum sensing in *Sinorhizobium meliloti*. J. Bacteriol. **187:**7931–7944.
14. **Jaeger, T., and C. Mayer.** 2008. The transcriptional factors MurR and catabolite activator protein regulate N-acetylmuramic acid catabolism in *Escherichia coli*. J. Bacteriol. **190:**6598–6608.
15. **Jiang, G. Q., A. H. Krishnan, Y. W. Kim, T. J. Wacek, and H. B. Krishnan.** 2001. A functional *myo*-inositol dehydrogenase gene is required for efficient nitrogen fixation and competitiveness of *Sinorhizobium fredii* USDA191 to nodulate soybean (*Glycine max* [L.] Merr.). J. Bacteriol. **183:**2595–2604.
16. **Karunakaran, R., et al.** 2009. Transcriptomic analysis of *Rhizobium leguminosarum* biovar viciae in symbiosis with host plants *Pisum sativum* and *Vicia cracca*. J. Bacteriol. **191:**4002–4014.
17. **Kawsar, H. I., K. Ohtani, K. Okumura, H. Hayashi, and T. Shimizu.** 2004. Organization and transcriptional regulation of *myo*-inositol operon in *Clostridium perfringens*. FEMS Microbiol. Lett. **235:**289–295.
18. **Kiss, G. B., E. Vincze, Z. Kalman, T. Forrai, and A. Kondorsi.** 1979. Genetic and biochemical analysis of mutants affected in nitrate reduction in *Rhizobium meliloti*. J. Gen. Microbiol. **113:**105–118.
19. **Kohler, P. R., J. Y. Zheng, E. Schoffers, and S. Rossbach.** 2010. Inositol catabolism, a key pathway in *Sinorhizobium meliloti* for competitive host nodulation. Appl. Environ. Microbiol. **76:**7972–7980.
20. **Kroeger, C., and T. M. Fuchs.** 2009. Characterization of the *myo*-inositol utilization island of *Salmonella enterica* serovar Typhimurium. J. Bacteriol. **191:**545–554.
21. **Lestrate, P., et al.** 2003. Attenuated signature-tagged mutagenesis mutants of *Brucella melitensis* identified during the acute phase of infection in mice. Infect. Immun. **71:**7053–7060.
22. **MacLellan, S. R., A. M. MacLean, and T. M. Finan.** 2006. Promoter prediction in the rhizobia. Microbiology **152:**1751–1763.
23. **Meade, H. M., S. R. Long, G. B. Ruvkun, S. E. Brown, and F. M. Ausubel.** 1982. Physical and genetic characterization of symbiotic and auxotrophic mutants of *Rhizobium meliloti* induced by transposon Tn*5* mutagenesis. J. Bacteriol. **149:**114–122.
24. **Meade, H. M., and E. R. Signer.** 1977. Genetic mapping of *Rhizobium meliloti*. Proc. Natl. Acad. Sci. U. S. A. **74:**2076–2078.
25. **Morinaga, T., H. Ashida, and K. Yoshida.** 2010. Identification of two *scyllo*-inositol dehydrogenases in *Bacillus subtilis*. Microbiology **156:**1538–1546.
26. **Oehler, S., M. Amouyal, P. Kolkhof, B. von Wilcken-Bergmann, and B. Mueller-Hill.** 1994. Quality and position of the three *lac* operators of *E. coli* define efficiency of repression. EMBO J. **13:**3348–3355.
27. **Pobigaylo, N., et al.** 2006. Construction of a large signature-tagged mini-Tn*5* transposon library and its application to mutagenesis of *Sinorhizobium meliloti*. Appl. Environ. Microbiol. **72:**4329–4337.
28. **Puukka, M.** 1973. Regulation of valine degradation in *Pseudomonas fluorescens* UK-1. Induction of enoyl coenzyme A hydratase. Acta Chem. Scand. **27:**718–719.
29. **Rossbach, S., and F. J. de Bruijn.** 2007. Transposon mutagenesis, p. 684–708. *In* C. A. Reddy (ed.), Methods for general and molecular microbiology, 3rd ed. ASM Press, Washington, DC.
30. **Rossbach, S., D. A. Kulpa, U. Rossbach, and F. J. de Bruijn.** 1994. Molecular and genetic characterization of the rhizopine catabolism (*mocABRC*) genes of *Rhizobium meliloti* L5-30. Mol. Gen. Genet. **245:**11–24.
31. **Saiz, L., and J. M. Vilar.** 2008. *Ab initio* thermodynamic modeling of distal multisite transcription regulation. Nucleic Acids Res. **36:**726–731.
32. **Sambrook, J., E. F. Fritsch, and T. Maniatis.** 1989. Molecular cloning: a laboratory manual, 2nd ed. Cold Spring Harbor Laboratory Press, Cold Spring Harbor, NY.
33. **Sorensen, K. I., and B. Hove-Jensen.** 1996. Ribose catabolism of *Escherichia coli*: characterization of the *rpiB* gene encoding ribose phosphate isomerase B and of the *rpiR* gene, which is involved in regulation of *rpiB* expression. J. Bacteriol. **178:**1003–1011.
34. **Steele, M. I., D. Lorenz, K. Hatter, A. Park, and J. R. Sokatch.** 1992. Characterization of the *mmsAB* operon of *Pseudomonas aeruginosa* PAO encoding methylmalonate-semialdehyde dehydrogenase and 3-hydroxyisobutyrate dehydrogenase. J. Biol. Chem. **267:**13585–13592.
35. **Streeter, J. G.** 1987. Carbohydrate, organic acid, and amino acid composition of bacteroids and cytosol from soybean nodules. Plant Physiol. **85:**768–773.
36. **Sundaram, T. K.** 1972. *myo*-Inositol catabolism in *Salmonella typhimurium*: enzyme repression dependent on growth history of the organism. J. Gen. Microbiol. **73:**209–219.
37. **Wood, M., and A. P. Stanway.** 2001. *myo*-Inositol catabolism by *Rhizobium* in soil: HPLC and enzymatic studies. Soil Biol. Biochem. **33:**375–379.
38. **Yamamoto, H., M. Serizawa, J. Thompson, and J. Sekiguchi.** 2001. Regulation of the *glv* operon in *Bacillus subtilis*: YfiA (GlvR) is a positive regulator of the operon that is repressed through CcpA and *cre*. J. Bacteriol. **183:**5110–5121.
39. **Yebra, M. J., et al.** 2007. Identification of a gene cluster enabling *Lactobacillus casei* BL23 to utilize *myo*-inositol. Appl. Environ. Microbiol. **73:**3850–3858.
40. **Yoshida, K., et al.** 2008. *myo*-Inositol catabolism in *Bacillus subtilis*. J. Biol. Chem. **283:**10415–10424.
41. **Yoshida, K. I., D. Aoyama, I. Ishio, T. Shibayama, and Y. Fujita.** 1997. Organization and transcription of the *myo*-inositol operon, *iol*, of *Bacillus subtilis*. J. Bacteriol. **179:**4591–4598.
42. **Yoshida, K. I., T. Shibayama, D. Aoyama, and Y. Fujita.** 1999. Interaction of a repressor and its binding sites for regulation of the *Bacillus subtilis iol* divergon. J. Mol. Biol. **285:**917–929.
43. **Zhang, Y. X., L. Tang, and C. R. Hutchinson.** 1996. Cloning and characterization of a gene (*msdA*) encoding methylmalonic acid semialdehyde dehydrogenase from *Streptomyces coelicolor*. J. Bacteriol. **178:**490–495.